Global features of quiet time counterelectrojet observed by Ørsted

Geeta Vichare[1,2] and R. Rajaram[1]

Received 4 January 2010; revised 15 October 2010; accepted 20 January 2011; published 12 April 2011.

[1] The present work investigates the reverse equatorial electrojet signature seen in the Ørsted satellite data, during magnetically quiet conditions. We found that whenever the satellite sees the reverse electrojet signature over the Indian region, it is always accompanied by the counterelectrojet (CEJ) at Indian observatories, and therefore, the reverse electrojet signature at the satellite height can be considered a proxy for the CEJ observed on the ground. Then using satellite observations, global features of the CEJ phenomenon are obtained. The broad features of the phenomenon such as a seasonal variation of the CEJ occurrence frequency, and also its anticorrelation with the normal electrojet strength, are found to be in agreement with earlier ground-based studies. Satellite-based investigations have a distinct advantage over ground data for studying the global extent as well as the longitudinal variation of the CEJ occurrence. It is observed that in general, the longitudinal extent of the phenomenon is very narrow, often restricted to less than 25°. However, the present analysis suggests that strong westward currents generated at a given universal time can result in CEJ at wider longitudinal locations. The percentage of CEJ occurrence is found to be highest in the Brazilian sector, between 300°E and 330°E longitude. It is observed that the CEJ is prone to occur where the magnetic declination is large, highlighting the role of the geometry of the ambient geomagnetic field. The present study emphasizes that the CEJ occurs more favorably when and where the strength of the normal equatorial electrojet is weak.

Citation: Vichare, G., and R. Rajaram (2011), Global features of quiet time counterelectrojet observed by Ørsted, *J. Geophys. Res.*, *116*, A04306, doi:10.1029/2009JA015244.

1. Introduction

[2] The reverse equatorial electrojet, better known as the equatorial counterelectrojet (CEJ) was first detected as a reversal of the horizontal magnetic field near local noon at Addis Ababa by *Gouin* [1962]. It was later found to occur rather frequently in the early morning or late afternoon hours [*Gouin and Mayaud*, 1967]. Although this phenomenon has been studied extensively for the last several decades, it remains enigmatic as it is yet to be understood in terms of physical processes. The westward currents manifesting during the reversal of the normal equatorial electrojet, may be explained in terms of atmospheric tidal effects [*Somayajulu et al.*, 1993; *Sridharan et al.*, 2002]. It is traditionally believed that an appropriate combination of tidal modes (particularly (1, −2), (2, 2), (2, 4)) would be able to generate the westward current at the magnetic equator [*Stening*, 1977; *Raghavarao and Anandarao*, 1980]. However, the narrow longitudinal extent of the CEJ occurrence [*Kane*, 1973; *Rastogi*, 1974] does not support the role of the migrating tidal winds in the generation of CEJ and hence one has to rethink the causative mechanism of the CEJ phenomenon. There is another stream of thought that the daytime equatorial electrojet currents can be modulated by the vertical wind shears either due to the interactions between height varying winds [*Reddy and Devasia*, 1981; *Rangarajan and Rastogi*, 1993] or by the interaction of gravity waves [*Vineeth et al.*, 2007]. *Stening et al.* [1996] was first to report the dependence of CEJs on high-latitude stratospheric warming events, which was recently confirmed by *Sridharan et al.* [2009]. The sudden stratospheric warming at high latitudes can be considered to generate semidiurnal tides that propagate cross equatorially to the other hemisphere [*Yamashita et al.*, 2002].

[3] The characteristics of the daytime counterelectrojets, which include solar cycle, seasonal, longitudinal, day-to-day variations of CEJs and also their dependence on lunar phase, have been illustrated extensively using ground magnetometer data. It has been observed that the phenomenon occurs more frequently in the morning hours (near 0700 LT) and in the afternoon hours (around 16 LT) [*Rastogi*, 1974; *Fambitakoye and Mayaud*, 1976]. Some of the well-established characteristics include its anticorrelation with solar activity [*Rastogi*, 1974; *Mayaud*, 1977; *Marriott et al.*, 1979] and normal equatorial electrojet (EEJ) strength [*Rastogi*, 1974]. *Mayaud* [1977] found that the morning CEJ is more frequent at the equinoxes, and afternoon CEJs are more during local summer solstice. The influence of lunar phase on the CEJ occurrence is reported by *Marriott et al.* [1979] and *Sastry*

[1]Indian Institute of Geomagnetism, Navi Mumbai, India.
[2]Formerly Geeta Jadhav.

0148-0227/11/2009JA015244

Table 1. LT Range of Satellite Passes During Each Month

Month	LT
April 1999	1345–1330
May 1999	1320–1259
June 1999	1250–1232
July 1999	1230–1215
August 1999	1200–1148
September 1999	1131–1112
October 1999	1103–1042
November 1999	1038–1015
December 1999	1005–0948
January 2000	0938–0924
February 2000	0914–0859
March 2000	0847–0825

and Jayaker [1972]; whereas *Bhargava et al.* [1980] found that the effect is restricted only for the winter season. On the other hand, *Rangarajan and Rastogi* [1993] found no such association of noontime CEJs with lunar tidal oscillations. Attempts have also been made to study the latitudinal extent of the reversal and found that the phenomenon is restricted over latitudes close to the magnetic equator [*Rastogi*, 1991; *Bhargava et al.*, 1980; *Onwumechili and Akasofu*, 1972]. Several studies have reported the association of CEJ phenomenon with the solar flares [*Rastogi et al.*, 1975, 1999; *Manju et al.*, 2009]. Additionally, it has been well established that the CEJ events are very well connected to the disappearance of *E* region irregularities and the reversal of ionospheric drifts [*Fambitakoye et al.*, 1973; *Rastogi*, 1974].

[4] Thus, CEJ phenomenon has been unraveled mainly through ground-based observations; in contrast very few attempts have been made to study the CEJ using low-altitude satellites. Using magnetic measurements of the X and Z components from Magsat data, *Cohen and Achache* [1990] observed that the ionospheric currents are eastward at dusk but westward at dawn; suggesting that CEJ effect was most of the time measured at dawn (80% of the days). Later, *Langel et al.* [1993] pointed out that the EEJ description obtained from Magsat data is biased by the necessary use of a main field model and concluded that the CEJ effect was not really observed in the Magsat dawn data. After inspecting POGO data, *Cain and Sweeney* [1973] reported 3 days indicating reverse EEJ signature. But *Onwumechili* [1985] argued that the reverse signature could result from the satellite flying immediately below a current layer additional to the classical electrojet flowing at 107 km altitude.

[5] The lack of consistency in the satellite-based CEJ results obtained by earlier workers is not entirely unexpected as they were based either on the Magsat satellite, which was located in the dawn-dusk orbit, or on the POGO satellite with highly elliptical orbits. For the satellite-based study of CEJ, it is desirable to have satellite passes with clear daytime global coverage at low altitude. Satellites like CHAMP, SAC-C and Ørsted are more suitable for such studies, as they all are near polar orbiting satellites covering good span of daytime. Using magnetic field measurements obtained from these satellites, *Tomas et al.* [2008] reported formation of the CEJ in the wake of the solar eclipse. *McCreadie* [2004] classified the EEJ signal observed in the scalar magnetic field measurements by Champ satellite into four categories. She reported CEJ as one of the categories, which occur only at certain longitudes viz., near 60°, 165°, 255° and 345° E. In the present communication, we investigate the CEJ signature seen in the Ørsted data in more detail, by first authenticating the CEJ signature seen at the satellite altitude through the use of simultaneous ground observations. Section 2 discusses the data selection and the subsequent treatment. Section 3 illustrates satellite passes showing CEJ events in the Indian longitude zone along with the ground observations from the same longitudinal belt. In addition to this, we also discuss a few cases that are just outside the Indian region.

[6] Since more than 70% of the area covered by the dip equator lies in the oceanic region, the study of the longitudinal extent of the CEJ phenomenon as well as its longitudinal variation using ground data is not possible. Only satellite data is capable of providing global coverage of the phenomenon. Therefore in the present study, we utilize the Ørsted data to obtain a global picture of the CEJ phenomenon. Section 4 examines the longitudinal extent of the CEJ, while a statistical study of seasonal, local, and zonal variation of the CEJ occurrence is made in section 5. The relation of longitudinal variation of CEJ occurrence to electrojet strength and geomagnetic field is discussed in section 6. Section 7 summarizes and discusses the results.

2. Data Selection and Treatment

[7] CEJ is known to occur during magnetically disturbed [*Kikuchi et al.*, 2003] as well as during magnetically quiet conditions [*Rastogi*, 1974; *McCreadie*, 2004]. In this paper we have analyzed about 60 days of scalar magnetic field (F) measurements taken by Ørsted satellite, which mainly include first 5 quiet days of each month (with $Ap \leq 8$) for the period between April 1999 and March 2000. The Ørsted satellite orbit is a near polar one, with a small drift with respect to the local time (−0.88 min per day). Table 1 shows the ranges of dayside local time (LT) for the satellite passes chosen during each month. Thus, during the period of present analysis, Ørsted covers local time ranging from 0825 to 1345 in the dayside hemisphere and hence constitutes a good data set for the study of the CEJ. However, the data set has a limitation that the satellite traverses did not encompass the late afternoon CEJ.

[8] For the main field subtraction, we use the CHAOS model [*Olsen et al.*, 2006]. This model employs static field coefficients up to order 50 and linear secular variation of degree 18. This model considers the effects of the magnetospheric ring current, tail current and induced currents as well.

[9] One should note that the localized eastward currents flowing in the *E* region give rise to normal equatorial electrojet (EEJ) phenomenon, which produces a southward magnetic field above the current system. Therefore at the satellite altitude (~700 km for Ørsted), the normal EEJ signature has ∨-shaped latitudinal profile, with a minimum at the dip equator accompanied by "shoulders" of increased field on either sides [*Jadhav et al.*, 2002]. On the other hand, the CEJ can be expected to have ∧-shaped profile with maximum near the dip equator at the satellite altitude.

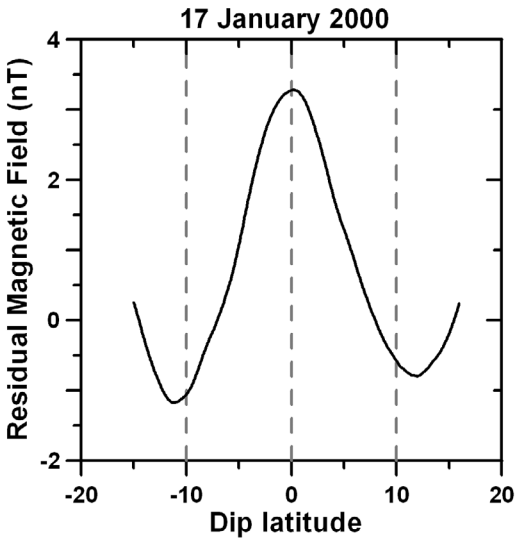

Figure 1. A typical reverse equatorial electrojet signature seen at Ørsted altitude.

Thus, when ∧ shape is observed in the residual magnetic field at the satellite height, we consider that as the reverse EEJ signature [*McCreadie*, 2004]. A typical reverse EEJ signature obtained at satellite height on 17 January 2000 is shown in Figure 1.

[10] As discussed in the introduction, some suspicions have been expressed on the reliability of the reverse EEJ signature observed by the satellite as an indicator of a CEJ event. Hence there is a need to critically examine the satellite records and ground geomagnetic measurements simultaneously, and to establish a one-to-one correspondence between the satellite signature of reversed EEJ and the CEJ observed on the ground. This is discussed in section 3.

3. Comparison of Reverse EEJ Signature Observed by Satellite With Underneath Ground Observations

[11] Here we present a few satellite traverses showing reverse EEJ signature, in the Indian geographic longitude zone between 50°E and 80°E. We compare these passes with the Indian ground observations. It is believed that the difference in the horizontal magnetic field component between an electrojet and a nonelectrojet station is a better indicator of the EEJ/CEJ [*Bhargava et al.*, 1980; *Rastogi*, 1974]. Therefore the EEJ index, which is obtained by subtracting the mean midnight level corrected horizontal magnetic field component measured at Alibag from that at Trivendrum is used here. Note that for the Indian region (75° EMT), Trivendrum (Dip Latitude 0.7°S, Geographic longitude 76.9°E) is considered as a near equatorial station and Alibag (Dip Latitude 9.8°N, Geographic Longitude 72.9°E) is considered just outside the influence of the equatorial electrojet. The EEJ indices for the Indian zone are routinely computed at Indian Institute of Geomagnetism, Navi Mumbai, India. It should be noted that earlier *Jadhav et al.* [2002] have found excellent correlation between the estimates of normal EEJ strength using ground observatory data and those obtained from the Ørsted magnetic field observations in Indian and American region.

[12] Figure 2 shows the magnetic field observations on 22 May 1999. Plots on the left hand side show the latitudinal profile of the magnetic field variations obtained from the Ørsted satellite measurements during two successive passes, which are over the Indian longitude zone. The longitude and universal time (UT) shown for each satellite pass indicate

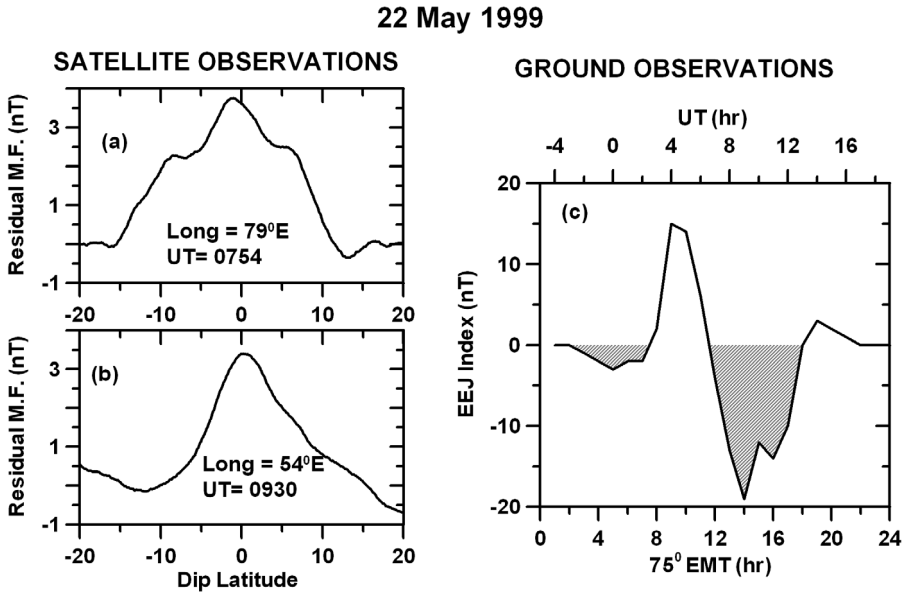

Figure 2. Event on 22 May 1999. (a and b) Latitudinal profile of the residual magnetic field observed by the satellite passes at different UTs and longitudes. (c) Hourly averaged value of EEJ strength (Trivendrum-Alibag) obtained from ground observations. Bottom axis in Figure 2c shows local time at 75°E longitude, while upper axis shows corresponding UT.

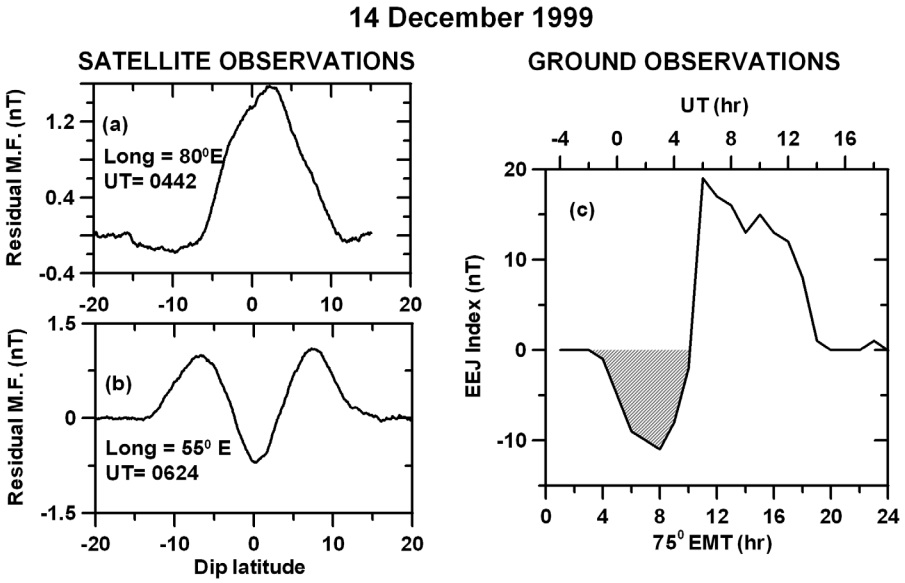

Figure 3. Same as Figure 2 but for event on 14 December 1999.

the values at the dip equator crossing. The plot on the right hand side shows the diurnal variation of the EEJ index, which is based on the ground observations in the Indian zone on the same day. Negative values of the EEJ index are shown by the shaded area. The bottom x axis shows local time (LT) at 75°E meridian, while the upper axis shows the corresponding UT. It is observed from the right hand side plot (Figure 2c) that the EEJ index goes below the nighttime level during afternoon hours (1200–1800 LT); the maximum depression is noted ≈20 nT and thus indicative of intense westward jet currents. The advantage of selecting a narrow longitudinal belt near Indian longitude is that the local times at ground and satellite locations are almost the same at a given UT. The corresponding UT range during which CEJ occurred at Indian stations is 0700–1300 UT. Now let us examine the satellite observations. Satellite pass at 0754 UT along 79°E longitude (Figure 2a) is just above Trivendrum and it shows the occurrence of CEJ. Thus for the same longitude and time, both satellite and ground identify the presence of CEJ. The next consecutive satellite pass (Figure 2b) that falls in the Indian longitude zone: 54°E at 0930 UT, also shows CEJ signature. It is interesting to note that the UT of this satellite pass lies within the UT range of CEJ observed by Indian ground stations. Thus, this pass is again in agreement with the ground observations. Therefore, the satellite and ground data observe the CEJ event simultaneously and give consistent results in the Indian zone.

[13] Figure 3 displays an event on 14 December 1999. Similar to Figure 2, the left side plots show satellite passes over the Indian zone and the right hand side shows the EEJ index computed using the Indian observatory data. The EEJ index shows morning CEJ until 1000 LT (corresponding UT is 0500 h). Here note that the small negative values of the EEJ index before sunrise ending up as a clear morning CEJ event is a typically observed feature at many longitudinal zones [*Mayaud*, 1977]. The satellite pass over Indian observatories, along 80°E longitude at 0442 UT (Figure 3a), shows CEJ signature and hence is found to be consistent with the ground observations. The next satellite pass at 0624 UT with 55°E longitude (Figure 3b) reveals normal EEJ signature; concurrently, ground data (Figure 3c) also shows an absence of CEJ by not showing a negative value

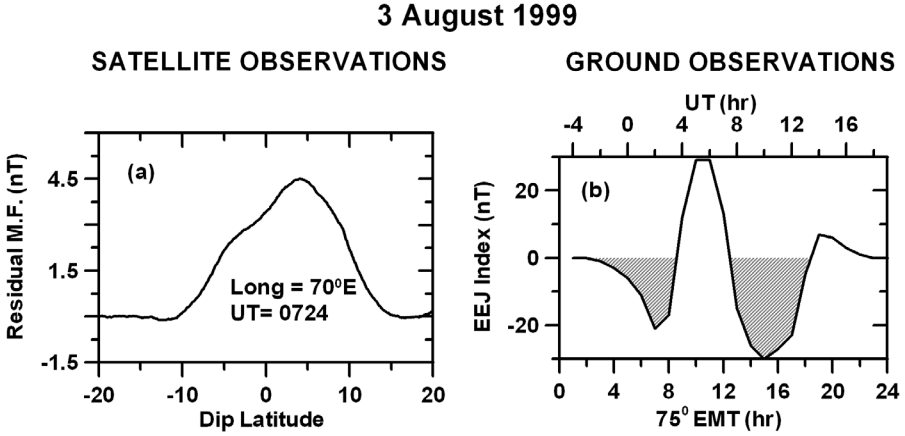

Figure 4. Same as Figure 2 but for event on 3 August 1999.

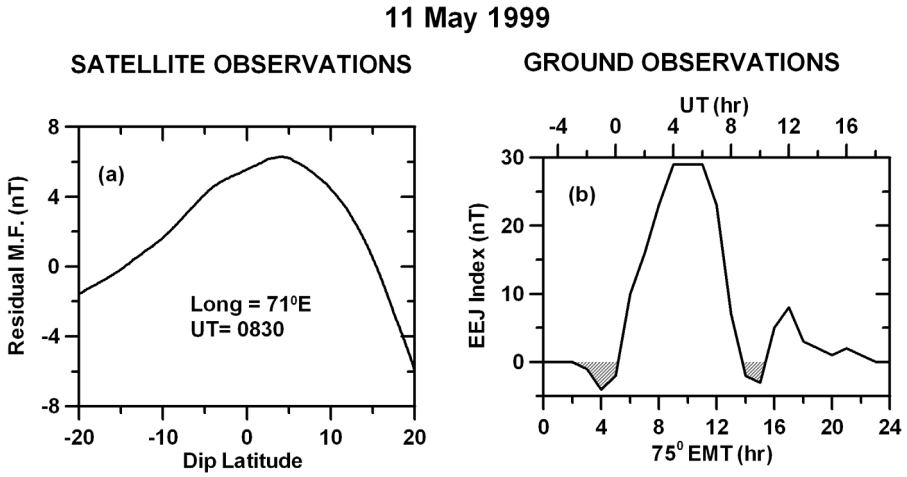

Figure 5. Same as Figure 2 but for event on 11 May 1999.

of EEJ index at that time, but it should be noted that the strength of EEJ at the satellite (~1.8 nT) and ground (~17 nT at 1124 LT) is very weak. Thus satellite and ground observations are in agreement.

[14] Figure 4 shows the event on 3 August 1999. Ground data (Figure 4b) shows a depression of the EEJ index below nighttime level in the morning as well as in the afternoon hours. The afternoon CEJ (between 0700 and 1300 UT) is very strong and goes up to −30 nT. Satellite pass at 0724 UT with 70°E longitude (Figure 4a) exhibits CEJ signature, and thus is in accordance with the ground observations. The next satellite pass at 0900 UT with longitude equal to 45°E, which is just outside the Indian zone (not shown in Figure 4), does not show the reverse electrojet signature, but exhibits very weak EEJ strength (~1.5 nT).

[15] Further, Figure 5 indicates the observations on 11 May 1999. Figure 5b shows the afternoon CEJ near 1500 LT (0830–1030 UT). Even though the afternoon CEJ seen by the ground observatories is weak (<−5 nT), the satellite pass over the Indian region along 71°E longitude, at 0830 UT, shows a CEJ signature, and thus concurrence is found between the ground and satellite observations. However, the next consecutive satellite pass (not shown here), which is outside the Indian zone, along 46°E at 1010 UT does not show reversed EEJ signature, suggesting a possible longitudinal constraint upon the reversed EEJ event.

[16] On 10 August 1999 (Figure 6b), Indian stations observe a strong afternoon CEJ effect (~−30 nT), during 0730–1030 UT. Consistent to this, the satellite pass at 0748 UT along longitude of 63°E exhibits reverse EEJ characteristics (Figure 6a). The next satellite pass at 0920 UT along 38°E, does not show reverse EEJ signature, but the amplitude of the EEJ signal is very weak (~1 nT). Note that the UT of this particular satellite pass lies within the UT range of CEJ phenomenon seen by the Indian observatories.

[17] Next, Figure 7a depicts one more CEJ case observed by the satellite in the Indian region on 30 June 1999 at 0830 UT. However, the variation of the EEJ index (Figure 7b) does not show negative values in the afternoon hours, but shows some depression, which is different than the normal EEJ variation. This anomaly becomes more obvious when compared with the expected normal electrojet pattern shown

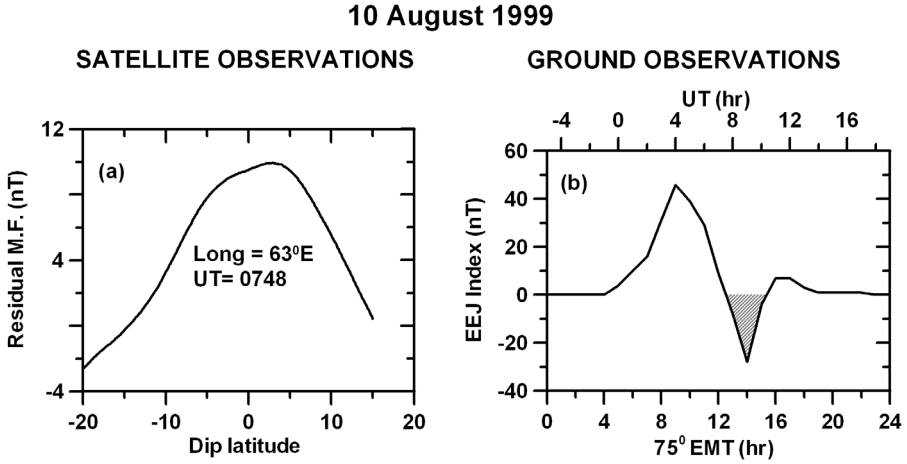

Figure 6. Same as Figure 2 but for event on 10 August 1999.

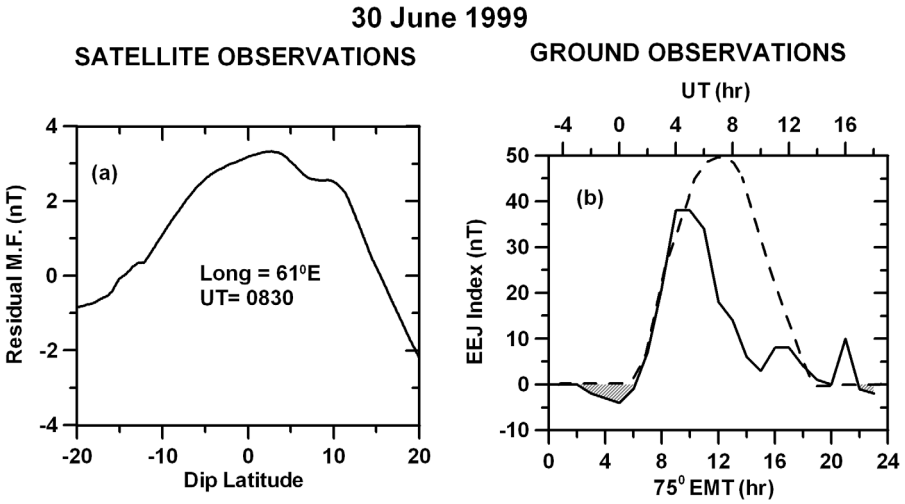

Figure 7. (a and b) Same as Figure 2 but for event on 30 June 1999. The dashed curve in Figure 7b indicates normal EEJ variation.

by a dashed curve in Figure 7b. This can indicate the presence of the westward current (characteristic of the CEJ), in additional to the normal eastward current system. This event takes place just after the local noon, when the normal eastward currents are stronger. The superimposed westward current might not be sufficiently strong to result in the net westward current, so we observe only the depression in the EEJ index instead of a proper CEJ event with negative values of the EEJ indices. Even this situation can be considered as an indicator of the CEJ phenomenon [*Rastogi*, 1974]. Similar situation is also observed on 14 June 1999, when the satellite pass over Indian region shows CEJ event, and the ground-data-based EEJ index shows the depression in the EEJ index, which can also be envisaged as CEJ.

[18] Extending this description further, we propose that the standard CEJ event (EEJ index below nighttime level) can be identified at a given location only if, the additional westward current to the normal daytime eastward current, is sufficiently strong to produce net westward current. If the local time at a given location is near noon, then it is required to have very strong westward current to produce net westward current, i.e., negative value of the EEJ index. On the other hand, during morning or evening times, the normal eastward current is weak and hence moderate westward current is sufficient enough to produce net reverse signature. This can result in more frequent occurrence of CEJ during morning and evening times, compared to times of strong eastward current near local noon. Therefore, it can be realized that the identification of the CEJ event depends on the local time at a given location.

[19] Now let us revisit our observations during earlier events (Figures 4, 5, and 6), where we have mentioned about the satellite passes just outside the Indian region. We found in Figures 4 and 6 that strong CEJ observed at Indian stations are not simultaneously accompanied by CEJ just outside Indian zone, rather satellite observations show very weak EEJ. During these satellite passes, the local times of the satellite were near noon, and at the same time the Indian observatories were in the afternoon sector. This suggests that the westward currents which are sufficient to produce a net westward current in the afternoon hours, are not sufficiently strong to result in a net westward current when relatively stronger eastward currents flow near local noon; but reduces the strength of the eastward currents, resulting in the weak EEJ at the satellite location. Thus the CEJs observed at the Indian observatories are simultaneously evident by the satellite passes little near but not directly inside the Indian zone and hence may suggest the role of the UT-dependent contribution in the development of the CEJ phenomenon. During the weak afternoon CEJ event on 11 May 1999 (Figure 5), we observed that the satellite pass with longitude just outside the Indian zone but within the UT range of CEJ seen at the Indian stations, records EEJ strength >3 nT which is not an abnormally weak EEJ at ~700 km altitude, and hence may not indicate the effect of a westward current system. Note that during 11 May, at 1010 UT, the LT at Indian station is 1510, while that at 46°E longitude is ~1310; and therefore the weak westward current capable to produce net westward current at ~1500 LT may not be strong enough to reverse or significantly reduce the stronger eastward currents flowing at ~1300 LT.

[20] Thus, here we have clearly demonstrated that if the satellite is in the longitude belt of the ground station, then the reversed EEJ recorded by the satellite is accompanied by the CEJ signature at the ground station. On some occasions, we notice that the CEJ seen by the satellite is accompanied by the depression in the EEJ index, which can also be visualized as an indicator of a westward current. Hence the reversed EEJ signature at the satellite height can be used as a proxy for the CEJ in the Indian sector and in what follows we assume that this holds for all longitude zones. During this exercise we also noticed that the stronger CEJs at Indian stations have influence outside the Indian region. Here it should be noted that the magnitude of the negative values of the EEJ index cannot be the only measure to determine the strength of the CEJ. It also depends on the local time; for example, the smaller values of negative EEJ index near local noon may comprise stronger westward current compared to larger negative values in the early morning or evening times. Consequently, the strong westward currents

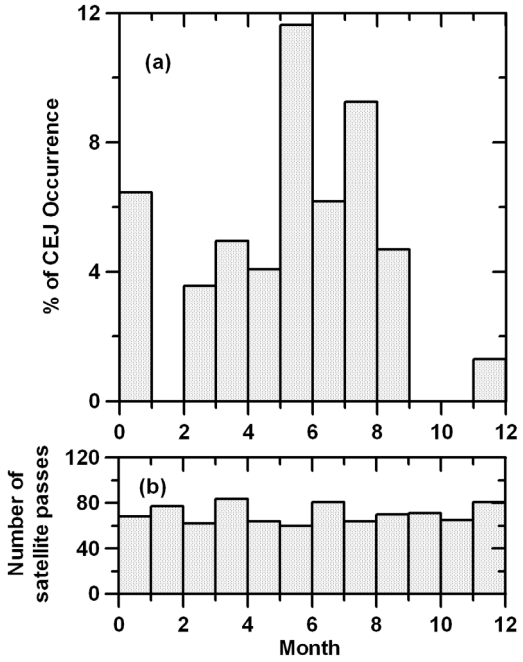

Figure 8. Seasonal variation of (a) CEJ occurrence frequency and (b) total number of quiet time satellite passes in each month.

generated at a given UT can result in CEJs at wider longitudinal locations with different local times, and thus the role of UT-dependent component in the development of the CEJ events is presented.

4. Longitudinal Extent of CEJ

[21] There have been suggestions based on the ground data that CEJs have a small longitudinal extent of 2 h or less [*Kane*, 1973; *Rastogi*, 1974]. They examined the cases of various CEJ events at different longitudes and found that the depressions of the horizontal component at these longitudes are varying in nature and concluded the limited longitudinal extent of the phenomenon. This has however been referred by *Mayaud* [1977] with the counterargument that limited longitudinal coverage may be responsible for arriving at such conclusions and CEJ as a rule may be 5–8 h in longitudinal extent. *Onwumechili and Akasofu* [1972] reported the occurrence of the CEJ over a wider longitude on some occasions. Traditionally, it is believed that the CEJ is due to the migrating atmospheric tides, and if this is true then it should be observed at all the longitudes at the same local time. Therefore, Ørsted satellite provides an ideal situation to examine this, as for a given day all the satellite passes along all the longitudes have almost the same local time. Our present satellite-based analysis indicates that the CEJ is never seen beyond three successive passes. During the present investigation of 60 quiet days, we notice that the expansion of CEJ occurrence to three consecutive passes is observed only once, whereas two successive passes are evident on four occasions. The maximum number of CEJ events (77%) were confined to only one pass. Therefore, only on rare occasions CEJ widens to the longitudinal extent of about 4 to 5 h. In general, only isolated satellite passes show CEJ and this narrows the longitudinal extent of the phenomenon to less than 25°. Therefore the natural conclusion is that, in general, CEJ has a narrow longitudinal extent of less than 2 h, which is consistent with the earlier ground-based findings of *Rastogi* [1974]. However, all this discussion is true if one believes that the CEJ is controlled solely by the migrating tides. But as mentioned in section 3, we have noticed a few cases, which suggest the role of UT-dependent contribution in the occurrence of the CEJ phenomenon. Hence one needs to inspect the signatures at all the longitudes (daytime) simultaneously, and find out how many consecutive longitudes observe the CEJ event, or at least have the influence of the westward current by weakening the normal EEJ strength. Using a single satellite, this type of study is not possible and requires multiple satellite observations.

5. Statistical Analysis

[22] For the present statistical study, we have identified each CEJ signature individually without resorting to any data manipulation required for automatic detection of the reversal. It is often observed that the latitudinal profile at satellite shows neither clear CEJ nor clear EEJ signature, i.e., no clear peak or trough at the dip equator. Rather it shows peak fairly away from the dip equator (~±5 to 10 deg). We call these as "non-EEJ" signatures, and in the present statistical analysis we do not judge these as CEJ signatures. It is also observed that "non-EEJ" signatures mostly occur in the longitude range from 300 to 340°E. It is interesting to note that in an independent satellite-based study of EEJ using Champ data, *McCreadie* [2004] also found this type of signature, which she classified as "No EEJ (NEJ)" and found to be more frequent near 345°E longitude at certain local times. It would be worth examining greater details of this feature in future using a larger database from multiple satellites. For the present analysis, we consider only clear signatures of CEJ, with peak near dip equator. We then compute the frequency of CEJ occurrence, defined as the ratio of total number of passes having CEJ signature to the total number of satellite passes.

5.1. Seasonal and Local Time Variation of CEJ Occurrence Frequency

[23] In order to establish the seasonal characteristics of the CEJ, it is necessary to have the same local time range for all the months. Satellite data with a limited time span is disadvantaged in this regard. The Ørsted satellite revolves around the Earth with a small drift with respect to the local time, which results in different local times during different months, as indicated in Table 1. Thus, for the presently analyzed data set of 1 year, local time variation is also sitting on the seasonal variation and vice versa. Figure 8a shows the frequency of the CEJ occurrence observed in each month. We see that the CEJ occurrence frequency maximizes in the month of June–August and a secondary peak occurs in January. It should be noted that even though December, January, and February have similar local time coverage between 0900 and 1000 LT (see Table 1), the January peak is distinctly larger. Also note that there is no single CEJ event reported in the months of February, October, and November. There could be doubts regarding

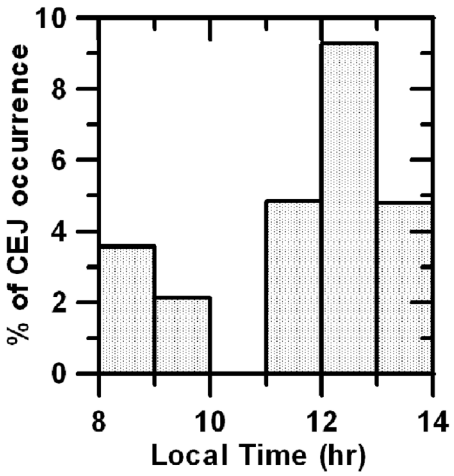

Figure 9. Local time variation of the CEJ occurrence.

the minima during these months, as one can argue that during spring and autumn months the geomagnetic activity is high [*Russell and McPherron*, 1973], and may not have a sufficient number of quiet time satellite passes. Therefore, we show the total number of quiet time satellite passes in each month in Figure 8b, and note that this quantity does not have any seasonal dependence. Quite a good number of satellite passes have been examined during the months without any CEJ events and thus substantiates the minimum occurrence of CEJ in those months.

[24] Figure 9 shows the local time variation of the CEJ occurrence frequency. It is expected to have a larger occurrence frequency away from the local noon, i.e., during early morning and evening hours. Due to limited span of data, it is not possible to examine the CEJ occurrence during the early morning (~0700 LT) or evening (~1600 LT) hours. But within the given local time coverage, we observe that the afternoon peak (1200–1300 LT) is larger than the morning (0800–1000 LT) peak. The local time range of 1200–1300 corresponds to the June–July solstice months. While December, January, February, and March months have LT range of 0800–1000, whose total CEJ occurrence frequency is less than that of June–July months (Figure 8a). Thus the higher occurrence frequency of CEJ during June–July is reflected in the local time variation. This demonstrates that in spite of the LT just after local noon, which is less favorable local time for the CEJ occurrence, a primary peak occurs in the month of June and hence the June peak is genuine. It is obvious to note minimum occurrence frequency of CEJ near 1100 LT, which is in accordance with ground-based observations [*Rastogi*, 1974]. Using Champ satellite observations, *McCreadie* [2004] also found similar seasonal and local time peaks.

5.2. Longitudinal Variation of CEJ Occurrence Frequency

[25] Using satellite data, it is possible to examine the longitudinal variation of CEJ, which otherwise is very difficult. The longitudes are divided into 12 sectors of width 30° each and the occurrence frequency is computed for each sector.

[26] Figure 10 shows the longitudinal variation of the percentage of CEJ occurrence frequency, along with the error bars (shown to the half of the scale for the sake of compactness) showing the 95% confidence interval about each percentage. The confidence interval is essentially a range within which the true value of a variable is thought to lie, with a specified level of confidence and is used to indicate the reliability of an estimate. Increasing the desired confidence level widens the confidence interval. They are closely related to statistical significance testing and extensively discussed in the literature [*Walpole*, 1968; *Smithson*, 2003].

[27] It should be noted that in the Brazilian sector, i.e., longitude zone between 300° and 330°E, the frequency of CEJ occurrence is the maximum. We observe that the peak in this longitude zone from 300° to 330°E is robust and appears even when we use an automated scheme for identification of CEJ events. The 95% confidence interval for this percentage peak ranges from 4.2% to 19.4%. The CEJ occurrence frequency is much less in the sectors adjacent to Brazilian area (1.5% in the sector 271°E–300°E and 3% for 331°E–360°E longitude bin). In order to examine the significance of the peak observed in the Brazilian region, we compare it with the adjacent sectors between 271°E and 360°E and found that the comparison meets the 95% criterion for the statistical significance.

[28] It should be noted that the secondary peaks lie in the Pacific region (150°–240°E longitude) and in the Indian region. If we clump together the three sectors between 150° and 240°E to represent Pacific region, then for the desired confidence level of 95%, the probability of CEJ occurrence can vary from 3.2% to 9.8%.

[29] It is exciting to note that using Champ satellite data *McCreadie* [2004] also observed more frequent occurrence of CEJ at certain longitudes close to the zones found in the present study. Thus the longitudinal variation of the CEJ occurrence resulted from the present study is in agreement with the results of the independent study using different

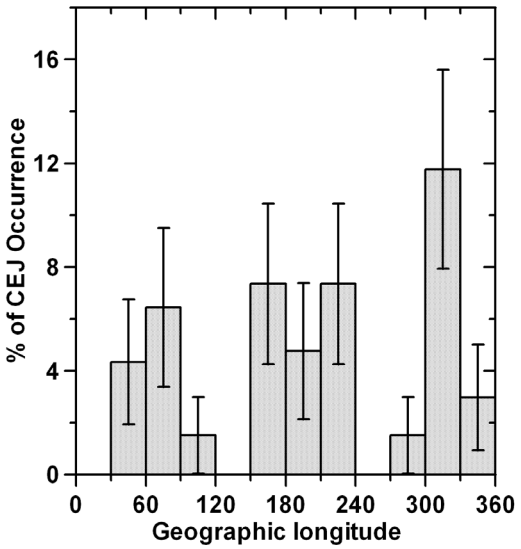

Figure 10. Longitudinal variation of CEJ occurrence frequency. Error bars indicate half of the 95% confidence interval.

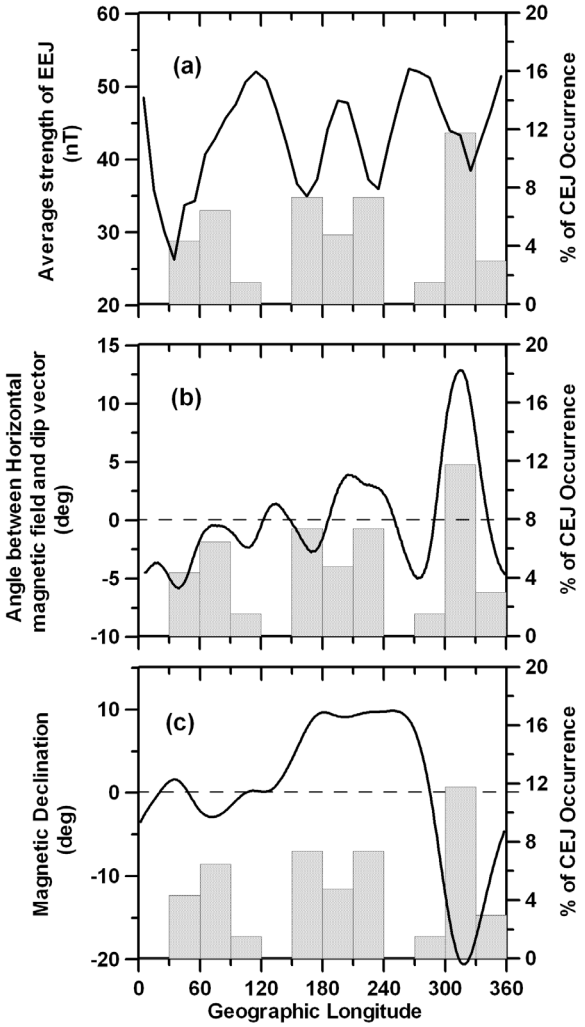

Figure 11. Longitudinal variation of various parameters at the dip equator, along with the CEJ occurrence frequency shown by the bar chart. (a) EEJ strength obtained from *Jadhav et al.* [2002], (b) angle between horizontal magnetic field and dip vector, and (c) geomagnetic field declination.

satellite for different time span, and hence supports its genuineness.

6. Relation of Longitudinal Variation of CEJ Occurrence to EEJ Strength and Geomagnetic Field

[30] In order to discover the parameter that controls the longitudinal variation of the CEJ incidents, we examine the zonal variation of various parameters. Figure 11 shows the longitudinal variation of various quantities at the dip equator, along with that of CEJ occurrence frequency (shown by the bar chart). Longitudinal variation of the EEJ strength (Figure 11a) is based on the Ørsted data collected during the same period as that of the present analysis, obtained by *Jadhav et al.* [2002]. Here, it should be noted that the longitudinal pattern obtained using the ground data may differ from that based on the satellite observations. It is possible to miss out some of the longitudinal peaks due to the limited coverage of the ground stations. Therefore, we choose to consider the longitudinal variation of the EEJ obtained using the same satellite and epoch. Figure 11a indicates that the EEJ strength and CEJ occurrence frequency are anticorrelated; that is, the frequency of CEJ occurrence is small in the zones where the EEJ strength is large and vice versa. This is in agreement with *Rastogi* [1974], who reported the largest occurrence of reversals at a station experiencing the weakest normal electrojet, which was later confirmed by many researchers [e.g., *Marriott et al.*, 1979].

[31] Figure 11b shows the longitudinal variation of the angle, α, between horizontal magnetic field and dip vector of ambient geomagnetic field. Here, we use IGRF 2000 coefficients and compute the characteristic values of geomagnetic field at the altitude of 105 km. The dip vector is defined as the normal drawn to the line of dip equator at a given longitude. In the EEJ models, the angle α, is tacitly assumed to be equal to zero even for the nondipolar magnetic field geometry of the Earth's magnetic field and hence zero line (dashed line) corresponds to the ideal geometry of the geomagnetic field. Figure 11b shows that at certain longitudes, the Earth's magnetic field significantly deviates from the assumed geometry, and the eastward currents flowing near the dip equator during daytime will not be exactly perpendicular to the ambient magnetic field. This could lead to an unconventional situation, which may result in the frequent development of the CEJ phenomenon. Therefore, here we examine the association of CEJ occurrence with the angle α. Figure 11b shows that the horizontal component of geomagnetic field makes largest angle of ~13° with the dip vector in the longitude zone from 300° to 330°E, where the CEJ occurrence frequency is maximum. Similarly in the longitude zone of 30°–60°E, 150°–180°E, and also near 210°E, the α angle deviates more from the zero value; and concurrently the CEJ occurrence is also greater. This may suggest that the CEJ occurrence frequency is proportional to the deviation from the idealized geometry, quantified by the magnitude of angle α. However, this dependence is not consistent in the Indian region (60–90°E) and American region (270–300°E). In the Indian sector, angle α is close to zero, yet CEJ occurrence frequency is significant. Whereas in the American region, the geomagnetic field deviates considerably from the ideal geometry ($\alpha \sim -5°$), but the CEJ occurrence is not so frequent. Therefore, though fairly good association is seen in some longitudinal zones, it is not observed at all longitudes.

[32] Next, in Figure 11c, we plot longitudinal variation of magnetic declination at the dip equator and the zero declination is shown by horizontal dashed line. The magnetic declination is the angle between magnetic north and geographic north. The declination is positive/negative when the magnetic north is east/west of geographic north. The tidal forcing, which is basically governed in the geographical coordinate system, plays very important role in the development of the *E* region dynamo, and hence one can guess that the large values of the declination angle may result in some anomalies in the dynamo action, which might lead to the favorable condition for the development of CEJ. Figure 11c shows that the magnitude of the declination angle primarily maximizes in the Brazilian sector (more than 20°), and next in the Pacific region (≈10°). Concurrently the

CEJ occurrence frequency also peaks in these regions. Again in the Indian sector, the value of declination is greater, which can be correlated to the peak observed in the CEJ occurrence frequency. Similarly, the declination is close to zero in the American region, African region and in 120°–150°E longitude zone, and correspondingly very rare occurrence of CEJ is seen in those regions. Thus a good correlation between CEJ occurrence frequency and the magnetic declination is evident. This suggests that the CEJ is more prone to occur in the region, where the magnetic north deviates greatly from the geographic north.

7. Summary and Discussions

[33] Present work delineates the characteristics of the global distribution of the counterelectrojet phenomenon, using satellite magnetometer data. By examining the magnetic field simultaneously at the satellite and Indian ground observatories, it has been demonstrated that the reverse EEJ signature at satellite represents the counterelectrojet. During this exercise, in order to minimize any complexities that may arise in the data interpretation because of large differences between satellite and ground station longitudes, only the satellite passes within the longitudinal band between 50°E and 80°E, which confirms that the satellite is over Indian zone are considered. Figures 2–7 display excellent correspondence between the satellite passes above Indian region and the ground observations. However, we also noticed that the strong afternoon CEJ seen at the Indian stations are simultaneously accompanied by the weak EEJ in the satellite passes just outside the Indian zone with near noon local times. We argue that the westward currents were strong enough to be able to reverse the late afternoon eastward currents at Indian stations, but were not strong enough to reverse the strong near local noon eastward currents at the satellite traverses. Hence although the signatures at the satellite were not completely reversed, the effect was seen through the reduced strength of the EEJ. The presence of additional westward currents that may be UT dependent adds up to the normal eastward current and produces the net effect at a given location. Hence, the present study implies a possibility of a UT-dependent source in the development of the CEJ phenomenon. We propose that at least on some occasions, the occurrence of the CEJ phenomenon depends on the strength of the universal time-dependent westward current system and also on the local time variations at a given location.

[34] Keeping in mind that improper removal of the Earth's magnetic field could lead to spurious results, it is very important to use a proper magnetic field model. In the present investigation, we have used the latest long-term main field model viz., CHAOS model [*Olsen et al.*, 2006], which is based on magnetic field data from Ørsted, CHAMP and SAC-C satellites for the period from March 1999 to the end of 2005. We also compared the results with the residual field obtained using Ørsted Initial Field Model (OIFM) [*Olsen et al.*, 2000], which was one of the very early satellite-based geomagnetic field models derived from Ørsted satellite data collected exclusively during the period of present analysis. Note that the OIFM model includes internal main field coefficients only to the order 13, secular changes to the order 8, an external field to degree 2, and *Dst*-dependent internal and external field correction up to degree 1. On the other hand in the case of the CHAOS model, the internal main field extends up to order 50 and secular variation up to 18. However, in the context of retrieving the CEJ signatures from Ørsted data, the OIFM appears to be adequate. This could imply that the crustal signatures make very little contribution at the Ørsted satellite height (~700 km).

[35] The seasonal and local time variations of the CEJ occurrence are found to be in accordance with the earlier ground-based results. The primary peak is observed in the month of June and a secondary peak in January; and also minimum CEJ occurrence near the local time of peak of the equatorial electrojet. Note that the months of June and January are near solstice months, when the EEJ strength is weak. This may suggest that the occurrence of CEJ is more likely to take place at the time of weak normal electrojet and the probability of CEJ occurrence is less when the EEJ is strong.

[36] To study the longitudinal extent of the CEJ, the ground database has several limitations. Due to mountains and oceans, it is not possible to have close longitudinal observations of the equatorial electrojet, which has really restricted our understanding of CEJ phenomenon. It has been suggested that some combination of diurnal and semidiurnal modes of tidal winds can account for the quiet day CEJ, with the semidiurnal term playing a more dominant role [*Forbes and Lindzen*, 1976; *Maeda*, 1977]. For migrating tide, one expects the CEJ signature to follow the sun and hence it is necessary to inspect the electrojet signature at the same local time at all longitudes. In this context the availability of the satellite data becomes valuable. It is seen that the CEJ is never seen beyond three successive passes, on a given day. Only on rare occasions, two to three consecutive passes showed CEJ signature, resulting in the longitudinal extent of about 4 to 5 h. Most of the times, only single satellite pass showed CEJ, which narrows the longitudinal extent of the phenomenon to less than 25°, which is consistent with the ground-based findings of *Rastogi* [1974]. Certainly, this observation indicates that the migrating atmospheric tides are not solely responsible for the CEJ occurrence. Perhaps, nonmigrating tidal components can play role in the formation of westward jet currents. Also the role of local wind shears in modifying the electrojet fields can be significant [*Reddy and Devasia*, 1981; *Vineeth et al.*, 2007]. The present study suggests a possibility of UT-dependent source in the development of the westward current system. And therefore any CEJ model should take recourse to include UT-dependent westward current source apart from the nonmigrating tidal and vertical wind shear effects. At this point it might not be possible to predict the additional sources of UT-dependent westward currents, but a wide guess could be due to the geomagnetic activity or solar flare effect. It would be appropriate to examine the longitudinal extent of the phenomenon at the same UT. This is not possible to investigate using single satellite observations. Upcoming Swarm mission with multiple low-orbiting satellites might be able to provide an opportunity to probe this aspect.

[37] Likewise, the satellite data is best suited for providing global zonal variation of the CEJ phenomenon. The present study reveals that the percentage of CEJ occurrence

is significantly largest in the Brazilian sector from 300°E to 330°E, and secondary peaks lie in Indian and Pacific region. An independent satellite-data-based study by *McCreadie* [2004] revealed similar longitudinal variation of the CEJ occurrence. Also many ground-based observations have confirmed the anomalous behavior of the equatorial ionosphere in the Brazilian sector [*Rastogi and Trivedi*, 2009; *Rastogi*, 2006; *Rastogi and Yumoto*, 2006; *Abdu et al.*, 1981].

[38] The present study establishes the anticorrelation between CEJ occurrence frequency and the EEJ strength, suggesting CEJ is more prone to occur in a region of weakest normal electrojet. This is again in accordance with our proposed description of the CEJ identification that for a given westward current system, the possibility of reversing the normal eastward currents is more at the locations of weak normal EEJ and vice versa. Hence it can be expected to observe anti correlation between the two.

[39] We observe that the CEJ occurrences are more frequent in the zones where the angle α, which is the angle between the horizontal component of the ambient magnetic field and the perpendicular drawn to the line of zero dip (the dip equator) is large. But we also perceive better correlation between the CEJ occurrence and the magnetic declination of ambient geomagnetic field.

[40] Certainly the physical significance of the regions of large declination angles, which to certain extent also correspond to regions with large α angles, lies in its anomalous geomagnetic field geometry. Figures 11b and 11c show that the angle α and declination change rapidly with the longitude. For example in the Brazilian sector angle α varies more than 10°/h and declination varies by ~20°/h. A simplistic picture based on the idea of the Earth rotating under a fixed sun synchronized ionospheric current system is significantly altered in these regions, as the dynamics that controls the evolution of the current circulation can be expected to be strongly controlled by such a spatially distorted magnetic field geometry. *Abdu et al.* [1981] have shown that the vertical ionization drift velocities in the evening equatorial *F* region over Jicamarca and Fortaleza, two stations located south of the geographic equator and separated by 30° in longitude in the American zone, present significantly different seasonal characteristics and the gross features of the spread *F* characteristics are indirectly dependent upon the magnetic field declination angle. Moreover, in the regions of strong declination changes there is bound to strong penetration of northern hemispheric current into the southern hemisphere and vice versa as the Sq current axis swings from east to west across the regions. Such movements can cause major topological changes in the current pattern in the regions of sharp spatial gradients, which can result in the favorable condition for the local reversal of the eastward currents.

[41] Finally the nonzero values of angle α indicate the regions where the ambient magnetic field direction is not perpendicular to the line of zero dip (the expected direction of EEJ current flow). This implies that the electrojet has significant current flows along the ambient magnetic field, which can modify the conventional electrojet current. These current flows along the ambient magnetic field are probably responsible for the variations in the declination component observed by *Rastogi and Trivedi* [2009] in the highly anomalous northeast Brazil sector. The tangential velocity gradients in the corresponding electron drifts with longitudinal gradients can be a potential source of local instabilities. One cannot rule out the possibility of triggering of Kelvin-Helmholtz type instability [*Chandrasekhar*, 1961] across the region leading the disruption or even a possible reversal of the currents locally.

[42] To conclude, the most important feature that comes out from the present analysis is that the CEJ is likely to occur when and where the normal EEJ is weak. In addition, we find that the CEJ occurs more frequently where the geometry of the ambient geomagnetic field differs from the idealized field geometry and also where local magnetic north differs from the geographic north by large angles. These features of the geomagnetic field make the normal EEJ current system complex. Hence, there is a need to include these aspects of the geomagnetic field in the modeling efforts of the counterelectrojet.

[43] **Acknowledgments.** We are grateful to the Ørsted Science Centre at the Danish Meteorological Institute for providing Ørsted satellite magnetic field data. We also thank the data processing staff of the Indian Institute of Geomagnetism for computing the EEJ indices.

[44] Robert Lysak thanks Heather McCreadie and the other reviewers for their assistance in evaluating this paper.

References

Abdu, M. A., J. A. Bittencourt, and I. S. Batista (1981), Magnetic declination control of the equatorial *F* region dynamo electric field development and spread *F*, *J. Geophys. Res.*, *86*(A13), 11,443–11,446.

Bhargava, B. N., N. S. Sastri, B. R. Arora, and R. Rajaram (1980), The afternoon counter electrojet phenomenon, *Ann. Geofis.*, *36*, 231–240.

Cain, J. C., and R. E. Sweeney (1973), The POGO data, *J. Atmos. Terr. Phys.*, *35*, 1231–1247, doi:10.1016/0021-9169(73)90021-4.

Chandrasekhar, S. (1961), *Hydrodynamic and Hydromagnetic Stability*, 481 pp., Oxford Univ. Press, Oxford, U. K.

Cohen, Y., and J. Achache (1990), New global vector magnetic anomaly maps derived from Magsat data, *J. Geophys. Res.*, *95*(B7), 10,783–10,800, doi:10.1029/JB095iB07p10783.

Fambitakoye, O., and P. N. Mayaud (1976), Equatorial electrojet and regular daily variation SR—II. The centre of the equatorial electrojet, *J. Atmos. Terr. Phys.*, *38*, 19–26, doi:10.1016/0021-9169(76)90189-6.

Fambitakoye, O., R. G. Rastogi, J. Tabbagh, and P. Vila (1973), Counterelectrojet and *Esq* disappearance, *J. Atmos. Terr. Phys.*, *35*, 1119–1126, doi:10.1016/0021-9169(73)90009-3.

Forbes, J. M., and R. S. Lindzen (1976), Atmospheric solar tide and their electrodynamic effects—I. The global S_q current system, *J. Atmos. Terr. Phys.*, *38*, 897–910, doi:10.1016/0021-9169(76)90073-8.

Gouin, P. (1962), Reversal of the magnetic daily variation at Addis Ababa, *Nature*, *193*, 1145–1146, doi:1038/1931145a0.

Gouin, P., and P. N. Mayaud (1967), A propos de l'existence possible d'un contre electrojet aux latitudes magnetiques equatoriales, *Ann. Geofis.*, *23*, 41–47.

Jadhav, G., M. Rajaram, and R. Rajaram (2002), A detailed study of equatorial electrojet phenomenon using Ørsted satellite observations, *J. Geophys. Res.*, *107*(A8), 1175, doi:10.1029/2001JA000183.

Kane, R. P. (1973), Comparison of geomagnetic changes in India and the POGO data, *J. Atmos. Terr. Phys.*, *35*, 1249–1252, doi:10.1016/0021-9169(73)90022-6.

Kikuchi, T., K. K. Hashimoto, T. I. Kitamura, H. Tachihara, and B. Fejer (2003), Equatorial counterelectrojets during substorms, *J. Geophys. Res.*, *108*(A11), 1406, doi:10.1029/2003JA009915.

Langel, R. A., M. Purucker, and M. Rajaram (1993), The equatorial electrojet and associated currents as seen in Magsat data, *J. Atmos. Terr. Phys.*, *55*, 1233–1269, doi:10.1016/0021-9169(93)90050-9.

Maeda, K. (1977), Conductivity and drifts in the ionosphere, *J. Atmos. Terr. Phys.*, *39*, 1041–1053, doi:10.1016/0021-9169(77)90013-7.

Manju, G., T. K. Pant, C. V. Devasia, S. Ravindran, and R. Sridharan (2009), Electrodynamical response of the Indian low-mid latitude ionosphere to the very large solar flare of 28 October 2003—A case study, *Ann. Geophys.*, *27*, 3853–3860, doi:10.5194/angeo-27-3853-2009.

Marriott, R. T., A. D. Richmond, and S. V. Venkateswaran (1979), The quiet time equatorial electrojet and counter electrojet, *J. Geomagn. Geoelectr.*, *31*, 311–340.

Mayaud, P. N. (1977), The equatorial counter-electrojet: A review of its geomagnetic aspects, *J. Atmos. Terr. Phys.*, *39*, 1055–1070, doi:10.1016/0021-9169(77)90014-9.

McCreadie, H. (2004), Classes of the equatorial electrojet, in *Earth Observation With CHAMP Results From Three Years in Orbit*, edited by C. Reigbar et al., pp. 401–406, Springer, Berlin.

Olsen, N., et al. (2000), Ørsted initial field model, *Geophys. Res. Lett.*, *27*(22), 3607–3610, doi:10.1029/2000GL011930.

Olsen, N., H. Lühr, T. J. Sabaka, M. Mandea, M. Rother, L. Tøffner-Clausen, and S. Choi (2006), CHAOS—A model of the Earth's magnetic field derived from CHAMP, Ørsted, and SAC-C magnetic satellite data, *Geophys. J. Int.*, *166*(1), 67–75, doi:10.1111/j.1365-246X.2006.02959.x.

Onwumechili, C. A. (1985), Satellite measurements of the equatorial electrojet, *J. Geomagn. Geoelectr.*, *37*, 11–36.

Onwumechili, C. A., and S. I. Akasofu (1972), On the abnormal depression of S_q(H) under the equatorial electrojet in the afternoon, *J. Geomagn. Geoelectr.*, *24*, 161–173.

Raghavarao, R., and B. G. Anandarao (1980), Vertical winds as a plausible cause for equatorial counter electrojet, *Geophys. Res. Lett.*, *7*(5), 357–360, doi:10.1029/GL007i005p00357.

Rangarajan, G. K., and R. G. Rastogi (1993), Longitudinal differences in magnetic field variations associated with quiet day counter electrojet, *J. Geomagn. Geoelectr.*, *45*, 649–656.

Rastogi, R. G. (1974), Westward equatorial electrojet during daytime hours, *J. Geophys. Res.*, *79*(10), 1503–1512, doi:10.1029/JA079i010p01503.

Rastogi, R. G. (1991), Latitudinal extent of the equatorial electrojet effects in the Indian zone, *Ann. Geophys.*, *9*, 777–783.

Rastogi, R. G. (2006), Sq and sfe currents at equatorial stations along the western and eastern African sectors, *Earth Planets Space*, *58*, 1475–1478.

Rastogi, R. G., and N. B. Trivedi (2009), Asymmetries in the equatorial electrojet around N-E Brazil sector, *Ann. Geophys.*, *27*, 1233–1249, doi:10.5194/angeo-27-1233-2009.

Rastogi, R. G., and K. Yumoto (2006), Equatorial electrojet in the east Brazil anomaly region, *Earth Planets Space*, *58*, 103–106.

Rastogi, R. G., M. R. Deshpande, and N. S. Sastri (1975), Solar flare effect in equatorial counter electrojet current, *Nature*, *258*, 218–219, doi:10.1038/258218a0.

Rastogi, R. G., B. M. Pathan, D. R. K. Rao, T. S. Sastry, and J. H. Sastri (1999), Solar flare effects on the geomagnetic elements during normal and counter electrojet periods, *Earth Planets Space*, *51*, 947–957.

Reddy, C. A., and C. V. Devasia (1981), Height and latitude structure of electric fields and current due to local east-west winds in the equatorial electrojet, *J. Geophys. Res.*, *86*(A7), 5751–5767, doi:10.1029/JA086iA07p05751.

Russell, C., and R. McPherron (1973), Semiannual variation of geomagnetic activity, *J. Geophys. Res.*, *78*(1), 92–108, doi:10.1029/JA078i001p00092.

Sastry, N. S., and R. W. Jayaker (1972), Afternoon depression in horizontal component of the geomagnetic field at Trivendrum, *Ann. Geofis.*, *28*, 584–591.

Smithson, M. (2003), *Confidence Intervals*, *Quant. Appl. in the Soc. Sci. Ser.*, vol. 140, Sage, Belmont, Calif.

Somayajulu, V. V., L. Cherian, K. Rajeev, G. Ramkumar, and C. R. Reddi (1993), Mean winds and tidal components during counter electrojet events, *Geophys. Res. Lett.*, *20*(14), 1443–1446, doi:10.1029/93GL00088.

Sridharan, S., S. Gurubaran, and R. Rajaram (2002), Structural changes in the tidal components in the mesospheric winds as observed by the MF radar during afternoon counter electrojet events, *J. Atmos. Sol. Terr. Phys.*, *64*, 1455–1463, doi:10.1016/S1364-6826(02)00109-8.

Sridharan, S., S. Sathishkumar, and S. Gurubaran (2009), Variabilities of mesospheric tides and equatorial electrojet strength during major stratospheric warming events, *Ann. Geophys.*, *27*, 4125–4130, doi:10.5194/angeo-27-4125-2009.

Stening, R. J. (1977), Magnetic variations at other latitudes during reverse equatorial electrojet, *J. Atmos. Terr. Phys.*, *39*, 1071–1077, doi:10.1016/0021-9169(77)90015-0.

Stening, R. J., C. E. Meek, and A. H. Manson (1996), Upper atmospheric wind systems during reverse equatorial electrojet events, *Geophys. Res. Lett.*, *23*(22), 3243–3246, doi:10.1029/96GL02611.

Tomas, A. T., H. Luhr, M. Rother, C. Manoj, N. Olsen, and S. Watari (2008), What are the influences of solar eclipses on the equatorial electrojet?, *J. Atmos. Sol. Terr. Phys.*, *70*, 1497–1511, doi:10.1016/j.jastp.2008.05.009.

Vineeth, C., T. K. Pant, C. V. Devasia, and R. Sridharan (2007), Highly localized cooling in daytime mesopause temperature over the dip equator during counter electrojet events: First results, *Geophys. Res. Lett.*, *34*, L14101, doi:10.1029/2007GL030298.

Walpole, R. E. (1968), *Introduction to Statistics*, pp. 193–196, Macmillan, New York.

Yamashita, K., S. Miyahara, Y. Miyoshi, K. Kawano, and J. Ninomiya (2002), Seasonal variation of non-migrating semidiurnal tide in the polar MLT region in a general circulation model, *J. Atmos. Sol. Terr. Phys.*, *64*, 1083–1094, doi:10.1016/S1364-6826(02)00059-7.

R. Rajaram and G. Vichare, Indian Institute of Geomagnetism, Plot 5, Sector 18, New Panvel, Navi Mumbai 410206, India. (vicharegeeta@gmail.com)